New insights into pb5, the receptor binding protein of bacteriophage T5, and its interaction with its Escherichia coli receptor FhuA

Ali Flayhan, Frank Wien, Maïté Paternostre, Pascale Boulanger, Cécile Breyton

Research paper

New insights into pb5, the receptor binding protein of bacteriophage T5, and its interaction with its *Escherichia coli* receptor FhuA

Ali Flayhan [a,b,c,d], Frank Wien [e], Maïté Paternostre [f,g], Pascale Boulanger [h], Cécile Breyton [a,b,c,d,*]

[a] CEA, Institut de Biologie Structurale Jean-Pierre Ebel, Grenoble, France
[b] CNRS, UMR5075, Grenoble, France
[c] Université Grenoble 1, France
[d] Institut de Biologie Physico-Chimique, CNRS, Université Paris-7, UMR7099, Paris, France
[e] Synchrotron SOLEIL, L'Orme des Merisiers, 91192 Gif-sur-Yvette Cedex, France
[f] CEA, Institut de Biologie et de Technologies de Saclay, CEA, CNRS, F-91191 Gif-sur-Yvette, France
[g] CNRS, UMR 8221, CEA-Saclay, F91191 Gif-sur-Yvette, France
[h] Institut de Biochimie et de Biophysique Moléculaire et Cellulaire, Université Paris-Sud-11, UMR CNRS 8619, Orsay, France

ARTICLE INFO

ABSTRACT

The majority of bacterial viruses are bacteriophages bearing a tail that serves to recognise the bacterial surface and deliver the genome into the host cell. Infection is initiated by the irreversible interaction between the viral receptor binding protein (RBP) and a receptor at the surface of the bacterium. This interaction results ultimately in the phage DNA release in the host cytoplasm. Phage T5 infects *Escherichia coli* after binding of its RBP pb5 to the outer membrane ferrichrome transporter FhuA. Here, we have studied the complex formed by pb5 and FhuA by a variety of biophysical and biochemical techniques. We show that unlike RBPs of known structures, pb5 probably folds as a unique domain fulfilling both functions of binding to the host receptor and interaction with the rest of the phage. Pb5 likely binds to the domain occluding the β-barrel of FhuA as well as to external loops of the barrel. Furthermore, upon binding to FhuA, pb5 undergoes conformational changes, at the secondary and tertiary structure level that would be the key to the transmission of the signal through the tail to the capsid, triggering DNA release. This is the first structural information regarding the binding of a RBP to a proteic receptor.

© 2012 Elsevier Masson SAS. All rights reserved.

1. Introduction

Bacterial viruses, bacteriophages, represent the widest group of biological entities on the planet [1]. They have co-evolved with bacteria, turning into virulent killers or prophages, and as such, they have a major impact on the ecology and evolution of their hosts [2]. More than 95% of known bacterial viruses belong to the order *caudovirales*: they have an icosahedral capsid containing a densely packed double-stranded DNA and a tail, a dynamic multiproteic assembly that serves to recognise the bacterial surface and deliver the genome into the host cell. The variable morphology of the tail has allowed the distinction of three families: Siphoviridae

(long non-contractile tail), Myoviridae (long contracting tail) and Podoviridae (short non-contractile tail) [3]. The host specificity is determined by the interaction of the Receptor Binding Proteins (RBPs), located at the tip of the tail, with defined receptor(s) at the surface of the bacterium (saccharides and/or proteins). This occurs most often in a two-step process, in which phages initially adsorb reversibly to low affinity receptors, prior to binding irreversibly to secondary sites or receptors [4]. The RBP-receptor interaction triggers conformational rearrangements within the tail structures, which induce capsid opening and cell wall perforation, allowing DNA release and transfer *via* the tail through the bacterial envelope [5,6]. Deciphering this cascade of events at a molecular level is a major issue for understanding the initial steps of infection.

The last decade has given insights into the structure of phage tail subcomplexes. It was shown that despite infecting different hosts Myoviridae coliphage T4 [5] and the Siphoviridae lactococcal phage p2 [7] share similar adsorption mechanisms. Other Siphoviridae, such as the *Bacillus subtilis* phage SPP1 and the coliphages λ and T5, require a specific protein receptor to irreversibly recognise and infect their host [4]. These phages exhibit a limited number of RBPs,

---

which are located in a unique central tail fibre whose structure remains to be elucidated. An important step in understanding the communication between the phage tail tip and capsid has come from SPP1. Electron microscopy has shown that the tail tip rearrangement following receptor binding of SPP1 to its receptor induces domino-type cascade conformational changes of the major tail protein through the tail towards the capsid [8,9].

The Siphoviridae coliphage T5 has proven to be a well-suited model to study phage−host interactions. Its 250 nm-tail ends with three L-shaped fibres attached to a conical baseplate and a straight central fibre [10]. Host recognition is initiated by reversible binding of the L-shaped fibres to the O-antigen of the lipopolysaccharide. The phage then binds irreversibly to the outer membrane iron-ferrichrome transporter FhuA by means of its RBP pb5 [11]. The crystal structure of FhuA has revealed a 22-stranded anti-parallel β-barrel and an N-terminal globular domain that folds inside the barrel and occludes it, referred to as the "cork" [12]. The external loops connecting the β-strands serve as binding sites for the natural substrate ferrichrome and other ligands of FhuA (phages T5, T1, Φ80, N15, HK02, the bacterial toxins Colicin M and Microcin J25, and the antibiotic albomycin) [13]. An interesting feature of T5 is that DNA release can be triggered in vitro in the external medium by the mere interaction of the virus with purified FhuA or into liposomes containing FhuA [14]. Furthermore, interaction between purified pb5 and FhuA yields a highly stable, stoichiometric complex, which is not denatured by 2% SDS unless heated to 70 °C [15]. This complex is currently the only complex biochemically available between an outer membrane receptor and a phage RBP. One of the major issues to elucidate the molecular mechanisms that propagate the signal from the RBP to the capsid is to describe the conformational rearrangements that initially take place between the RBP and its receptor. Here, we have further characterised the complex formed between pb5 and FhuA, and determined the strength of interaction between the two proteins. Attenuated total reflectance Fourier transform infrared spectroscopy (ATR-FTIR), near-UV and Synchrotron Radiation Circular Dichroism (SRCD) and limited proteolysis were used to characterise the conformational changes induced by the formation of the complex.

2. Materials and methods

Overexpression and purification − FhuA purification was carried out as described in [16], except that outer membranes were solubilised with 1% N,N dimethyl dodecylamine-N-oxide (LDAO), and the Nickel affinity (HiTrap Chel, 5 ml) and anion exchange (HiTrap Q, 1 ml) columns were performed in 0.1 and 0.05% LDAO, respectively. H_6-pb5 was overexpressed and purified as described in [15] with minor modifications: the Nickel affinity (HiTrap Chel, 5 ml) and cation exchange (HighTrap SP, 1 ml) columns were performed in 25 mM MES pH 6.0. All columns were from GE Healthcare. To remove NaCl, FhuA and pb5 were diluted 1000 times with 0.05% LDAO, 20 mM Tris pH 8.0 and with 20 mM MES pH 6.0, respectively, and re-concentrated by ultrafiltration on an AMICON 50 kDa cutoff. The FhuA-pb5 complex was formed by adding equimolar amounts of the two proteins, which results in 100% formation as described in [15]. This was check by performing analytical gel filtration chromatography (SD200 5/150), or SDS gel electrophoresis of 0.8:1, 1:1, 1:0.8 ratios of FhuA:pb5 that never show free protein at the 1:1 ratio. Prior to biophysical assays, all samples were spun at 12,240 g for 10 min at 4 °C to remove any particulate matter.

2.1. Surface plasmon resonance

Analyses were performed using BIAcore X and 3000 instruments. Pb5 was diluted to 24 μg/ml in 10 mM sodium acetate pH 5.0

and immobilised on the surface of a CM5 sensor chip (GE Healthcare) using the amine coupling chemistry (4200 RU). Binding of FhuA to immobilised pb5 (5400 RU after saturation of the surface) was measured at a flow rate of 20 μl/min in 10 mM Tris pH 8.0, 150 mM NaCl, 0.05% LDAO. Equivalent volumes of protein were injected over an activated-deactivated surface to serve as blank sensorgrams for subtraction of the bulk refractive index background. To regenerate the surface, i.e. to dissociate the complex, 20 μl of classical regenerating/dissociating agents containing 0.05% LDAO were injected at a flow rate of 20 μl/min. For Single Cycle Kinetics measurement, pb5 was diluted to 0.6 μg/ml, and 43 μl were injected at a flow rate of 5 μl/min, resulting in a low-density immobilisation of pb5 on the surface (670 resonance units). 250 μl of increasing concentrations of FhuA (0.5−8; 4−64 and 32−512 nM) were injected at a flow rate of 30 μl/min, with a dissociation time of 300 s.

2.2. SRCD

SRCD measurements of FhuA, pb5 and of the FhuA−pb5 complex were recorded on the DISCO beamline at SOLEIL Synchrotron [17]. All samples were loaded into the same 200 μm pathlength suprasil round cell (Hellma, Jena). Acquisitions (1 nm steps, 0.5 s integration) between 280 and 170 nm were performed in triplicates. Averaged sample spectra were subtracted from their corresponding buffer baseline (concentrator flow through) collected in the same cell. Spectral magnitudes were verified using a solution of (+)-camphor-10-sulphonic acid at 6.3 mg/ml in a 100-μm pathlength cell. Spectra were cut at the mid heigth of the High Tension voltage signals (800 V), which resulted in cutoff at 178 nm (Direct Current constant, High Tension variable). Final spectra were normalised to the respective peptide bond number and scaled to molar concentrations. FhuA (723 aminoacids), pb5 (662 aminoacids) and the FhuA-pb5 (1385 aminoacids) complex were 0.44, 0.56 and 1 mg/ml respectively, as determined from the UV absorption peak at 280 nm using a Nanodrop 1000 spectrophotometer. The extinction coefficients used were $\varepsilon_{280,FhuA} = 1.386 \, (mg/ml)^{-1} \, cm^{-1}$, $\varepsilon_{280,pb5} = 1.421 \, (mg/ml)^{-1} \, cm^{-1}$, $\varepsilon_{280,Complex} = 1.403 \, (mg/ml)^{-1} \, cm^{-1}$. The calculated spectrum of the FhuA−pb5 complex was obtained by summing the spectrum of FhuA and that of pb5 using the formula $[(\Delta\varepsilon_F \, X \, N_F) + (\Delta\varepsilon_p \, X \, N_p)]/(N_F + N_p)$, where the subscripts F and P indicate FhuA and pb5 respectively, and N is the number of peptide bonds in each protein [18]. Secondary structure determinations were obtained using the DICHROWEB server [19] with the CDSSTR analysis program and taking the SP175 as a dataset reference [20]. These results were cross-validated with the SELCON3 [21] analysis program.

2.3. Thermal denaturation

Full spectra were collected in triplicates, between 25 and 100 °C at 5 °C increment and 3 min equilibration for each temperature in 10 μm (FhuA, 7.93 mg/ml) and 200 μm (pb5, 0.56 mg/ml and the complex 1 mg/ml) suprasil round cells. Thermal spectral acquisitions followed the same protocol as above. For greater accuracy and proof of reproducibility, a second set of spectra was collected in quadruplets for FhuA (1.1 mg/ml), using 5 °C increment between 25 and 60 °C and 1 °C increment between 60 and 100 °C. Datasets were deconvolved to their basis curves and conformational weights, using the Convex Constraint Algorithm [22]. The evolution with temperature of the CD signal at 196, 197 and 218 nm were used to estimate the thermodynamics of unfolding of FhuA, pb5 and the complex, respectively. Data were fitted globally using non-linear regression fitting routines. For pb5, data were best fitted with a two-state unfolding transition of a monomer as described in [23].

Data of pb5 above 90 °C had to be omitted due to aggregation of the protein. For FhuA, data were fitted using a three-state transition model, with correction for pre- and post-transition linear changes in ellipticity as a function of temperature. Data was fitted with the following equation: $\theta_t = \alpha_F\theta_F + \alpha_I\theta_I + \alpha_U\theta_U$, where θ_t is the observed ellipticity at any temperature, α the mole fraction and θ the ellipticity, and the subscript F, I and U refer to the fully folded, the intermediate and the unfolded forms, respectively. Finally, for the complex, data were best fitted using a two-state transition model, between a folded dimer and unfolded monomers as described in [23]. Data was treated with SigmaPlot 8.0.

2.4. Near-UV CD

Near-UV CD spectra of FhuA, pb5 and of the FhuA-pb5 complex were recorded on a JOBIN YVON CD6 at 20 °C. All samples were loaded into the same 1 cm quartz cell. Acquisitions (1 nm step 2 s integration) between 240 and 320 nm were performed in triplicates. Averaged sample spectra were subtracted from their corresponding buffer baselines. Spectra were normalised to protein concentration (0.3–0.5 mg/ml) and pathlength. The calculated spectrum of the FhuA–pb5 complex was obtained by adding the normalised spectra of FhuA and pb5.

2.5. ATR-FTIR

Spectra were measured at 4 cm^{-1} resolution with a Bruker IFS 66 spectrophotometer equipped with a 45°n ZnSe ATR attachment. The buffer signal was removed by subtraction of the sample buffer (concentrator flow through) spectrum recorded before each measurement. FhuA and pb5 samples were in 20 mM Tris pH 8.0, ~200 mM NaCl, 0.1% LDAO and 25 mM MES pH 6.0, ~400 mM NaCl, respectively. Shown spectra resulted from the average of 30 scans, and were corrected for the linear dependence on the wavelength of the absorption measured by ATR. The spectra of each protein and of the complex were normalised to the area between 1550 and 1800 cm^{-1}, i.e. the amide I and II region, and by the mass of each protein. It has been checked that the contribution of LDAO is negligible in the Amide I-II region. To extract the different secondary structure determinants, the spectra (after subtraction of a linear baseline between 1590 and 1710 cm^{-1}) were decomposed into 4 Gaussian components using Peak Fit Software (4.12 version) and the residuals were minimised for each spectrum.

2.6. Proteolysis

Purified pb5, FhuA and the pb5-FhuA complex were incubated with trypsin (1/1200, 1/600, 1/300 w/w protease/pb5), chymotrypsin (1/500, 1/250, 1/125 w/w) subtilisin (1/500, 1/250, 1/125 w/w) for 40–50 min at room temperature. After the reaction, one half of the proteolysed proteins was mixed with its unproteolysed partner to generate the complex. Proteolysis reactions were then immediately stopped by the addition of 2% SDS, β-mercaptoethanol, heating for 2 min at 95 °C when appropriate, and immediate plunging into liquid Nitrogen. Samples were loaded on SDS-PAGE at 4 °C.

3. Results

3.1. Probing secondary structure changes upon FhuA–pb5 complex formation

SRCD is a powerful tool for the characterisation of the secondary structure content of proteins: i) it can resolve CD signals down to 168 nm in the far-UV region due to the high flux of the synchrotron light source, and ii) the signal-to-noise levels are greatly improved

when compared to in house CD. This allows high sensitivity, better spectral resolution, and ultimately improves the information content and the secondary structure prediction [24]. Fig. 1A and B shows the spectra of FhuA, pb5 and of the FhuA–pb5 complex. FhuA and pb5 display a large positive peak at 196–197 nm ($\pi \rightarrow \pi^*$) and a negative peak at 218–216 nm ($n \rightarrow \pi^*$), respectively, which are characteristic of β-sheets, and in agreement with published CD spectra [15,25,26]. The deconvolution into secondary structure identifies a content of 47%, 9%, 6%, 38% for FhuA and of 44%, 11%, 6%, 39% for pb5 of β-sheets, turns, α-helices and other structures, respectively. These proportions are compatible with the crystal structure of FhuA, and with secondary structure prediction of pb5 (Table 1). The lower intensity of the pb5 CD signal could indicate the presence of less structured regions. The spectrum of the FhuA–pb5 complex displays similarly two peaks, at 199 nm and 218 nm. The comparison of the measured spectrum of the FhuA–pb5 complex with the normalised sum of the individual spectra (calculated spectrum, see Methods) however shows clear differences (Fig. 1B). A shift of the maximum from 196 to 199 nm and an increase of the intensity of the signal, as well as a small change around 220 nm are significant and clearly distinguishable above the noise level. These differences indicate conformational changes and reorganisation at the secondary structure level within the proteins upon complex formation. Deconvolution reveals an increase of the β-sheet at the expense of all other structures (Table 1).

These results were further confirmed by ATR-FTIR. This technique also probes secondary structures of proteins. The analysis is focused on amide I vibrations (1600–1700 cm^{-1}), which mainly arise from the vibration stretching mode of the backbone carbonyl groups. The decomposition assigns wavenumbers to backbone carbonyl groups involved in different strengths and types of hydrogen bonds, and therefore secondary structure types [27,28]. In accordance with the literature, the absorption around
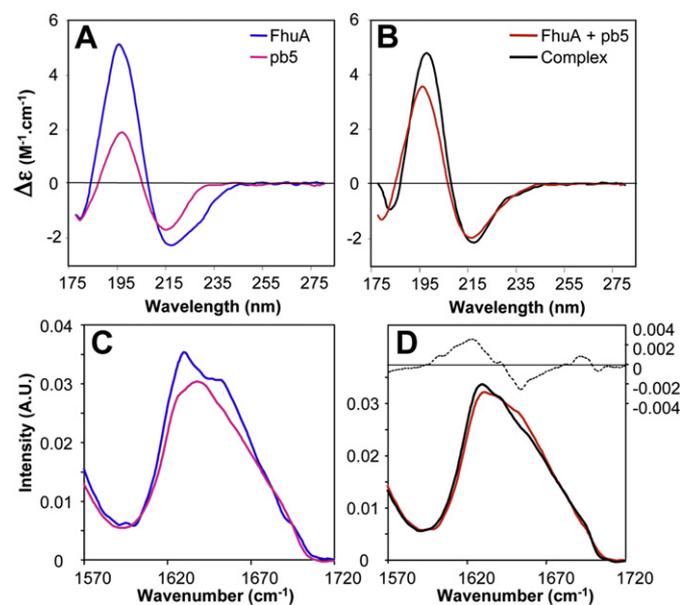
Fig. 1. SRCD (A,B) and ATR-FTIR (C,D) spectra of the isolated proteins and of the complex. A and C. FhuA (blue curve) and pb5 (pink curve). B and D. Comparison between the measured spectrum (black curve) and the calculated one (red curve) of the FhuA–pb5 complex. The calculated SRCD spectrum (B) was obtained by adding the spectrum of FhuA and that of pb5 normalised to the number of peptide bonds. In the case of FTIR (D), it was obtained by adding the spectrum of FhuA and that of pb5 normalised to the mass of each protein and to the area of Amide I and II region (1550–1800 cm^{-1}). Dotted curve: difference between the measured and the calculated spectra. AU: Arbitrary units.

Table 1

Analyses of the secondary structures of FhuA, pb5 and the FhuA—pb5 complex. Numbers are given in %. SRCD spectra were deconvolved using the DICHROWEB server [19] with the CDSSTR analysis program and taking the SP175 as a reference dataset. Pb5 sequence analysis was performed with the Garnier program [44]. FTIR spectra were decomposed into 4 Gaussian using peak Fit (see Fig. S1).
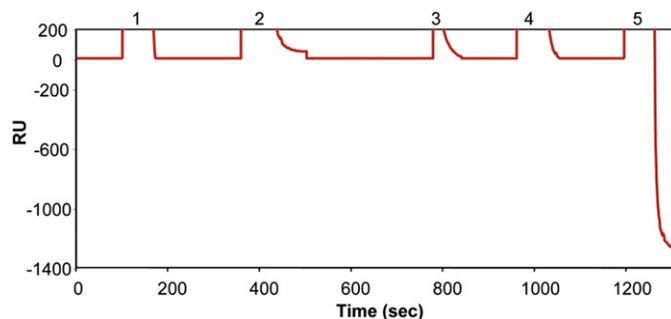
Protein	Method	β-sheet	Turn	α-helix	Other
FhuA	PDB (1QFG)	53	13	7	27
	CD [26]	38	12	17	33
	SRCD (rmsd = 0.018)	47	9	6	38
	FTIR	50	18	32	
pb5	Sequence prediction	40	24	7	28
	CD [15]	51	22	6	21
	SRCD (rmsd = 0.028)	44	11	6	39
	FTIR	44	24	32	
	SRCD (rmsd = 0.024)	52	8	4	36
Complex	SRCD calculated (rmsd = 0.028)	46	10	6	38

Fig. 2. SPR analysis of the FhuA-pb5 complex. A. Pb5 was immobilised on the chip onto which FhuA was injected, forming the complex (see Materials and Methods). Sensorgram of the raw signal after injection of classical denaturing reagents (20 μl at 20 μl/min). 1. 4 M NaCl, 2. 3 M MgCl₂, 3. 20 mM EDTA, 4. 4 M Guanidinium-HCl and 5. 6 M Guanidinium-HCl. All solutions contained 0.05% LDAO. R.U.: resonance unit.

$1635-1650$ cm^{-1} is assigned to random and α-helical conformations, the combination of absorption around $1615-1630$ and $1675-1685$ cm^{-1} to anti-parallel β-sheet structures, and the vibration around $1663-1670$ cm^{-1} to turn structures.

The ATR-FTIR spectra of FhuA and pb5 (Fig. 1C) confirm the high β-sheet content of both proteins. Indeed, their decomposition identified for FhuA 50%, 18% and 32% of β-sheet, -turn, and random and α structures, respectively, in very good agreement with the crystal structures (Table 1, Fig. S1). For pb5, respective % of 44, 24 and 32 are found, also in good agreement with the sequence prediction and the SRCD spectrum (Table 1). The comparison of the spectrum measured for the complex with that obtained by addition of the normalised spectra of FhuA and pb5 shows some substantial differences, witnessing secondary structure reorganisation upon complex formation (Fig. 1D). The subtraction of both spectra shows two positives peaks at 1623 and 1690 cm^{-1} that are characteristic for anti-parallel β-sheets and a negative peak at 1652 characteristic for random-α structures. Thus, upon complex formation, random-α structures are converted to β-sheet, in total agreement with the SRCD results.

### 3.2. The FhuA—pb5 complex is extremely stable

Real-time Surface Plasmon Resonance (SPR) experiments show that the complex between FhuA and pb5 has a very high affinity. The binding signal was not due to aggregation of FhuA on the surface, as the signal could be saturated (Fig. S2A), and no dissociation of the complex was detectable after either a night's wash, or treatments with classical dissociating agents (4 M NaCl, 3 M MgCl₂, 20 mM EDTA, 1 M Na₂SO₄, 4 M Guanidinium-chloride, 1 M diethylamine, 1% acetic acid, 10 mM Glycine pH 2.0, 25 mM HCl, or 100 mM NaOH) (Fig. 2). Dissociation of the complex was observed after injection of 6 M Guanidinium-chloride (Fig. 2), or 50 mM HCl, and was most probably the result of protein denaturation. Indeed, addition of FhuA on the regenerated surface, corresponding to dissociated pb5, did not result in new complex formation, suggesting that pb5 was no longer correctly folded. In order to measure the dissociation constant of the complex, Single Cycle Kinetics were performed [29]. This method involves sequentially injecting an analyte concentration series without any regeneration steps. However, at the high or low level of pb5 immobilisation and at the low FhuA concentrations tested, and with the presence of detergent in the running buffer, the detection limits of the Biacore 3000 were reached without the possibility of measuring either a k_{off} (i.e. dissociation of the complex following FhuA injection) or reaching an equilibrium during the injection time (i.e. reaching a plateau during the injection of FhuA) (Fig. S2B). Thus, the data could not be analysed either within a kinetic or in a thermodynamic frame, and

the K_d could not be calculated. Tentative determination of the k_{on} by fitting curves shown in Fig. S2A resulted in an upper limit of the K_d value of the order of a hundred of pM.

To further characterise the interaction between the two proteins, thermal denaturation of the proteins and the complex was probed by SRCD (Fig. 3). Analysis of the spectra of FhuA with Convex Constraint Algorithm [22] shows that three basis spectra are needed to reconstitute the whole dataset (Fig. S3A,D), indicating a three-state unfolding
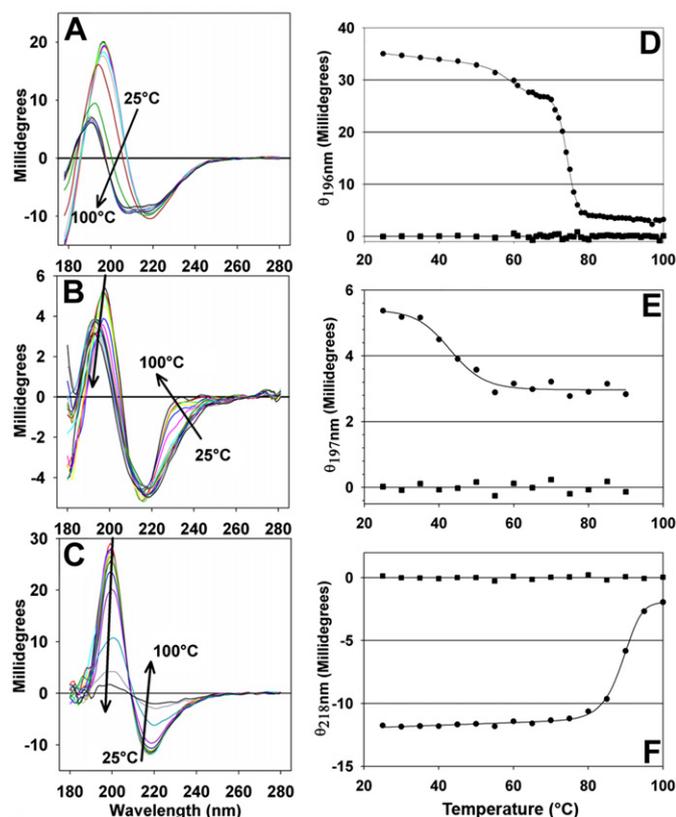
Fig. 3. SRCD thermal denaturation. A, B and C: Spectra of FhuA, pb5 and the complex, respectively, collected as a function of temperature. Data were collected at 5-deg increments with 3 min equilibration at each temperature. Black arrows show the evolution of the spectrum as the temperature increases. D, E and F: SRCD signal (circles) and fitted curves (solid line) for FhuA at 196 nm, pb5 at 197 nm and the complex at 218 nm, respectively. The raw data of FhuA were fitted with equations for the unfolding of a monomer with three-state model, that of pb5, with equations for the unfolding of a monomer with two-state model, and that of the complex for the unfolding of a dimer to unfolded monomers with two-state model. Squares represent the residuals from the model.

mechanism. Analysis of the basis spectra indicates that at around 65 °C, FhuA unfolds into a stable intermediate species characterised by the drop in the CD signal and the shift from 196 to 193 nm of the positive peak (27% β-sheet and 34% α-helix). Above 75 °C the unfolded state is characterised by a negative peak at 208 nm (12% β-sheet and 35% α-helix) (Fig. S3A). In agreement with a three-state unfolding mechanism, the CD signal of FhuA at 196 nm as a function of temperature is best fitted using a three-state model and shows two inflections points at 60 and 74 °C (Fig. 3D). For pb5 and the complex, only two basis spectra were needed to fit the SRCD thermal denaturation data (Fig. S3B,E and C,F), indicating that both pb5 and the complex follow a two-state unfolding mechanism. Analysis of the basis spectra indicates that denatured pb5 retains an overall β-strand (40%) conformation during thermal denaturation (Fig. S3B). Interestingly, within the complex, both proteins unfold cooperatively and lose almost all their secondary structures, as witnessed by the almost flat CD signal for the denatured complex (Fig. S3C). The unfolding not being reversible, unfolding enthalpies calculated from the fitting may not be relevant. However, calculation of unfolding Tm is independent of the reversibility of the reaction. The evolution of the CD signal at 197 nm for pb5 and 218 nm for the complex, as a function of temperature, are best fitted by equations describing a two-state unfolding mechanism, and provide unfolding Tm of 43 °C for pb5 and 89 °C for the complex (Fig. 3E,F). These results are in agreement with previous differential scanning calorimetry results [15,16], where the two transitions displayed by FhuA were attributed to the unfolding of the loops and cork at 65 °C and of the barrel at 74 °C. The large difference in the transition temperatures between the complex and the two isolated proteins indicates that the complex has a strong stabilising effect on both proteins. The fact that the first transition of FhuA, corresponding to the unfolding of the cork is not present in the complex suggests that pb5 also binds to the cork, or alternatively that pb5 binding to extracellular loops indirectly locks the cork in the barrel.

3.3. Aromatic residues environment changes upon formation of the FhuA–pb5 complex

Near-UV (250–320 nm) CD probes the overall tertiary structure of proteins, being sensitive to the environment and flexibility of aromatic side chains within the proteins: an intense signal witnesses a rigid structure and a well-folded protein. Fig. 4 shows the normalised spectra of FhuA (36F, 41Y, 9W), pb5 (26F, 31Y, 10W) and of the complex. Pb5 shows a rather broad spectrum with an indiscrete peak at 292 nm, and an important shoulder at 250–270 nm, suggesting a stronger contribution of tryptophans and phenylalanines, respectively. FhuA's spectrum is dominated by the contribution of tyrosines, with a peak centred around 280 nm. The comparison of the measured and calculated signal of the complex (Fig. 4B) shows a huge increase in the overall CD signal. The measured spectrum preserves the same shape as that of FhuA, dominated by the tyrosine contribution. These results strongly suggest that upon complex formation, the tertiary structure of the proteins becomes more rigid, and that the environment of aromatic residues are better defined, with a possible stacking of the latter at the interface between the two proteins. Indeed, the loops of FhuA count a rather large number of aromatics, especially tyrosines, which could be involved in interaction with pb5.
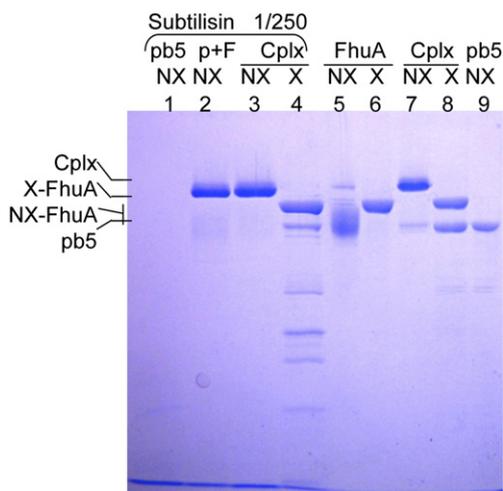
3.4. Proteolysis

Limited proteolysis revealed further evidence for the conformational changes occurring upon formation of the complex. Pb5 and FhuA were separately digested by subtilisin and then assayed for their ability to form a stable complex with their unproteolysed partner. A convenient means of assessing the FhuA–pb5 complex
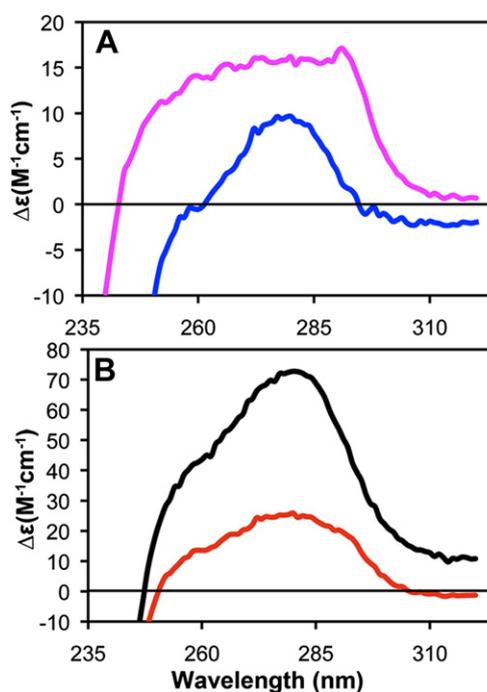
Fig. 4. CD spectra in the near-UV region of the isolated proteins and of the complex. A. Spectra of FhuA (blue curve) and pb5 (pink curve). B. Comparison between the measured (black curve) and calculated (red curve, sum of the normalised spectra of FhuA and pb5) spectra of the FhuA–pb5 complex.

formation is SDS gel electrophoresis as the FhuA–pb5 complex is not dissociated by SDS, and migrates as a unique band unless heated [15]. When incubated with subtilisin, pb5 undergoes extensive proteolysis, as attested by the absence of discrete bands on denaturing electrophoresis (Fig. 5, lane 1). Subtilisin being an a specific protease, proteolysis occurs randomly, leading to

Fig. 5. Gel electrophoresis analysis of proteolysed pb5 alone or in complex with FhuA. Lanes 1–4: proteolysed samples 50 min at room temperature with 1/250 (w/w) subtilisin/pb5. p + F: proteolysed pb5 to which was added stoichiometric amounts of FhuA prior to loading onto the gel, Cplx: preformed complex incubated with the protease. Lanes 5–9: control samples of FhuA, complex (Cplx) and pb5. Samples were either heated in the presence of 2% SDS (X) To fully denature the proteins, or non-heated (NX). As for all β-barrel proteins, non-heated FhuA is not completely denatured and migrates faster than the heated protein, as a smear. Non-heated complex is not denatured, the two proteins are not dissociated and migrate as a unique band, at a higher molecular weight than FhuA or pb5 (note the little excess of pb5 in the non-heated control complex). The heated complex is dissociated into the two proteins that migrate independently [15]. 10% acrylamide home-made gel.

a mixture of peptides of different length resulting in an "invisible smear" on the gel after denaturation of the protein by SDS. Strikingly, digested pb5 forms an SDS stable complex when mixed to FhuA (Fig. 5, lane 2). This is shown by the presence of a sharp band migrating at the same position as the complex (compare with lane 7). Only a very small amount of free FhuA is detected as a fuzzy band (compare with lane 5). This indicates that cleavage of pb5 in multiple sites does not alter the ability of the protein to form a stable complex with FhuA, suggesting that the domain that interacts with FhuA has conserved its three-dimensional structure. This hypothesis is confirmed by ATR-FTIR that shows that both proteolysed and untreated pb5 have identical spectra (Fig. S4B). Size exclusion chromatography further suggests that pb5 folds as a unique domain, as both untreated and digested pb5 elute at the same volume when loaded onto an SD200 column (Fig. S4C). We thus assume that pb5 adopts a very tight (but SDS sensitive) core structure, sensitive to proteolysis in external loops that do not or little affect the interaction with FhuA. FhuA is also rather sensitive to subtilisin, its tertiary structure however remaining unaffected (not shown). Proteolysis likely mainly occurs in the external loops, the transmembrane β-barrel of FhuA being shielded from the aqueous solution by the detergent belt. As in the case of pb5, these proteolysis events do not prevent the formation of the complex when unproteolysed pb5 is added to proteolysed FhuA (not shown). Thus, limited proteolysis of one or the other component does not impair the formation of the highly stable complex that is characterised by the unique band on SDS-PAGE.

When the complex is incubated with the same amount of subtilisin, no proteolysis bands are observed on the unheated sample (Fig. 5, lane 3). When heated, it shows intact or very poorly proteolysed FhuA (compare lane 4 with lane 6). This observation is consistent with previous studies highlighting the role of the large extracellular loops of FhuA in the irreversible binding of phage T5 [13]. These loops are likely protected from proteolysis in the complex, and the periplasmic turns are probably too short to be accessible to the protease. Conversely to FhuA, pb5 in the complex was proteolysed, as attested by the lower intensity of the pb5 band (compare lane 4 with lane 9), and by the presence of discrete bands of lower molecular weight. Importantly, when pb5 is complexed with FhuA, proteolysis is not as extensive as for isolated pb5. The same result was obtained with either twice as much or twice as little protease, indicating that pb5, when in complex with FhuA is much less sensitive to the protease. This can stem from protection of the interaction surface, and/or because pb5 is less flexible and/or because of conformational changes within pb5. When incubated with more specific proteases, *i.e.* trypsin and chymotrypsin, similar results are obtained, except that proteolysis of pb5 yields discrete bands on the gel (Fig. S4A). Furthermore, the proteolysis profile of pb5 alone or complexed with FhuA is identical with both proteases, suggesting that the surface of interaction between the two proteins represents a minor part of the surface of pb5, and does not affect the proteolysis profile.

4. Discussion

A striking feature of tailed bacteriophages is the strength of the interaction with their host receptor, which is considered as irreversible. Indeed, phage T5, once bound to the outer membrane protein FhuA by means of its RBP pb5, cannot be dissociated from its host. The FhuA–pb5 complex is to date the only receptor-RBP complex that has been reconstituted *in vitro*. Here we have used complementary biophysical and biochemical approaches to characterise the major determinants of the interaction between pb5 and FhuA, as well as the conformational changes occurring within the proteins.

4.1. Interaction between FhuA and pb5

The strength of the FhuA–pb5 interaction is attested by SPR experiments that show that the complex resists to treatments with classical dissociating agents, and that it could be dissociated only by 6 M Guanidinium-chloride or 50 mM HCl, most probably as the result of the denaturation of the two partners. Single Cycle Kinetics method allows to circumvent the regenerating step to measure the equilibrium constant K_d of very high affinity complexes [29]. In our experimental conditions, the detection limit was reached before attaining low enough FhuA concentrations to observe either an equilibrium during, or dissociation after, FhuA injection. An upper limit of the K_d was determined to be in the order of a hundred of pM, reflecting the very high affinity of FhuA for pb5. The tightness of the complex is correlated to an extreme thermal stability, with an unfolding temperature shifted to 89 °C, while FhuA and pb5 unfold at 60 and 43 °C, respectively. Intermolecular interactions thus stabilise each of the two proteins, and destabilisation of the complex likely occurs as a result of a loss of the secondary structure of both proteins.

Previous studies suggested that the external loops 4 [30] and 8 [13] of FhuA are involved in the binding of phage T5. The first transition of FhuA, at 60 °C, corresponding to unfolding of the cork, is absent in the complex. This suggests that in the complex, the cork domain of FhuA is stabilised and dependent on the rest of the complex, and thus that pb5 interacts with this domain as well as with the loops of the barrel. This is in agreement with the fact that even though T5 infects cells baring a FhuA mutant in which the cork domain has been deleted (FhuAΔ$_{21-128}$) [31], the affinity of binding of T5 to FhuAΔ is reduced with respect to binding to WT FhuA [16]. Thus, the interaction between FhuA and pb5 seems to involve a large area, including loops from the cork domain as well as loops of the barrel. Near-UV results also suggest an important contribution of aromatic residues stacking in the interaction. These observations can explain the high affinity between the two proteins and the large biochemical and thermal stability.

4.2. Conformational changes within the complex

Upon FhuA–pb5 interaction, significant conformational changes occur within the complex. More specifically, *i)* β structures are formed at the expense of all other secondary structures, as shown by SRCD and ATR-FTIR; *ii)* the tertiary structure of the complex appears more rigid, as shown by near-UV CD, and *iii)* proteolysis experiments clearly indicate conformational changes and/or structuration/rigidification throughout pb5 upon binding to FhuA. In addition, we note that whereas purified pb5 is poorly soluble (it precipitates at a concentration above 0.5 mg/ml, or in the presence of imidazol, of detergent, or in a dialysis tube), the FhuA–pb5 complex is soluble to at least 20 mg/ml. The interaction with FhuA could mask hydrophobic patches of pb5 exposed to the solvent, either at the interface between the two proteins, or within the protein through conformational changes/rigidification. Furthermore, from SRCD (low signal with respect to FhuA's signal) and proteolysis data, pb5 appears more structured when in complex than isolated.

Whereas no structural information is available on pb5, several FhuA structures have been determined either unliganded or with a variety of bound ligands on its extracellular side (ferricrocin, ferrichrome, phenylferricrocin, albomycin, and rifamycin) [32]. *In vivo,* these ligands are actively transported across the outer membrane in a TonB-dependent manner. Interestingly, none of the structures show secondary structure conformational changes upon ligand binding, apart from the unwinding of the small switch helix belonging to the cork domain, on the periplasmic side of the protein, allowing the binding information to reach TonB. Structure

comparison between the unliganded and the liganded protein only show rigid body movements of loops and of the cork. CD and FTIR data obtained on FhuA either free or bound to ferrichrome show very little spectral changes [26]. Furthermore, molecular dynamics performed on both FhuA and FhuA-ferrichrome show movements of the loops as rigid entities [33]. The FhuA structure thus appears very stable, and one can reasonably postulate that no secondary structure conformational changes will occur upon binding of pb5. Thus, it is reasonable to attribute the conformational changes observed by SRCD and ATR-FTIR solely to pb5. From the ATR-FTIR peak area, and from the decomposition of the SRCD spectra, this would correspond to ∼10–12% conversion of random-α-other structures to β-sheets within pb5.

4.3. Pb5 shares no common feature with other known RBPs

Common features of RBPs of known atomic structure include that *i*) they are present in moderate to high copy number in the phage particle (18–54), *ii*) they recognise oligosaccharide receptors, and *iii*) they fold into multiple domains. This is the case for the RBP of the lactococcal *Syphoviridae* phages p2 [34] and TP901-1 [35], which consist of a receptor-binding head domain, a N-terminal domain that anchors the protein to the phage, and a short and rigid neck domain that links both domains. Importantly, these domains appear to behave as independent and stable entities amenable to structural studies as shown for the RBP of the lactococcal phage bIL170 [36]. A multi-domain organisation is also a landmark of the RBP of the short tail fibres of the *Myoviridae* coliphage T4, the RBP of *Podoviridae* P22, Sf6 and HK620 as well as the RBP of the *Tectiviridiae* phage PRD1 (see [37] for a review).

The characteristics of phage T5 RBP appears however to differ from those of the above-mentioned phages. Pb5 binds a proteic receptor and is present at a low copy number in the phage (less than 3) [38]. Furthermore, our results indicate that pb5 probably folds as a unique domain. Indeed, although cleaved in multiple sites by proteolysis, isolated pb5 migrates at the same retention volume as the uncleaved protein on gel filtration, and forms a complex with FhuA that is not dissociated in SDS-PAGE. FhuA is also the receptor for the lambdoid phages T1, Φ80, N15 and HK022 [32]. Yet search for sequence homologies between pb5 and the putative RBP of these phages failed. On the other hand, alignment of pb5 with the RBP of the T5-related phages BF23 [39], H8 [40], EPS7 [41] and SPC35 [42] highlights strong sequence identity at the N-terminus and in patches scattered along the sequence (Fig. S5). Since these phages bind to different receptors, it is likely that the conserved sequences correspond to regions of the protein interacting with the rest of the phage, whereas regions with less homology would be specific for binding to the receptor. No clear domain could be delineated in these sequences, confirming the idea that the RBP of the T5-related phages would fold as a unique domain. Earlier studies suggested that pb5 is located at the top of the straight T5 fibre nearby the baseplate [43]. Yet, recent electron microscopy observations indicate that pb5 is most likely located at the very tip of the straight fibre (Zivanovic et al., in preparation). This raises the question of which of the other proteins of the straight fibre interact with pb5 and how they contribute in transmitting the conformational changes through the phage tail and potentially in DNA transport. This information would not only be of importance for understanding the atypical mechanism of transport of phage T5 DNA, but could also be relevant for phages belonging to the same family.

Acknowledgements

Appendix A. Supplementary material

Supplementary data related to this article can be found online at doi:10.1016/j.biochi.2012.05.021.

References

[1] H. Brüssow, R.W. Hendrix, Phage genomics: small is beautiful, Cell 108 (2002) 13–16.
[2] E. Hambly, C.A. Suttle, The viriosphere, diversity, and genetic exchange within phage communities, Curr. Op. Microbiol. 8 (2005) 444–450.
[3] H.W. Ackermann, Bacteriophage observations and evolution, Res. Microbiol. 154 (2003) 245–251.
[4] I.C. Vinga, São-José, P. Tavares, M.A. Santos, Bacteriophage entry in the host cell, in: G. Węgrzyn (Ed.), Modern Bacteriophage Biology and Biotechnology (2006), pp. 163–203.
[5] P.G. Leiman, P.R. Chipman, V.A. Kostyuchenko, V.V. Mesyanzhinov, M.G. Rossmann, Three-dimensional rearrangement of proteins in the tail of bacteriophage T4 on infection of its host, Cell 118 (2004) 419–429.
[6] A. Bertin, M. de Frutos, L. Letellier, Bacteriophage-host interactions leading to genome internalization, Curr. Opin. Microbiol. 14 (2011) 492–496.
[7] G. Sciara, C. Bebeacua, P. Bron, D. Tremblay, M. Ortiz-Lombardia, J. Lichiere, M. van Heel, V. Campanacci, S. Moineau, C. Cambillau, Structure of lactococcal phage p2 baseplate and its mechanism of activation, Proc. Natl. Acad. Sci. U S A 107 (2010) 6852–6857.
[8] C. Plisson, H.E. White, I. Auzat, A. Zafarani, C. São-José, S. Lhuillier, P. Tavares, E.V. Orlova, Structure of bacteriophage SPP1 tail reveals trigger for DNA ejection, EMBO J. 26 (2007) 3720–3728.
[9] A. Goulet, J. Lai-Kee-Him, D. Veesler, I. Auzat, G. Robin, D.A. Shepherd, A.E. Ashcroft, E. Richard, J. Lichiere, P. Tavares, C. Cambillau, P. Bron, The opening of the SPP1 bacteriophage tail, a prevalent mechanism in Gram-positive-infecting siphophages, J. Biol. Chem. 286 (2011) 25397–25405.
[10] Saigo K, Isolation of high-density mutants and identification of nonessential structural proteins in bacteriophage T5; dispensability of L-shaped tail fibers and a secondary major head protein, Virology 85 (1978) 422–433.
[11] K.J. Heller, Identification of the phage gene for host receptor specificity by analyzing hybrid phages of T5 and BF23, Virology 139 (1984) 11–21.
[12] A.D. Ferguson, E. Hofmann, J.W. Coulton, K. Diederichs, W. Welte, Siderophore-mediated iron transport: crystal structure of FhuA with bound lipopolysaccharide, Science 282 (1998) 2215–2220.
[13] F. Endriss, V. Braun, Loop deletions indicate regions important for FhuA transport and receptor functions in *Escherichia coli*, J. Bacteriol. 186 (2004) 4818–4823.
[14] P. Boulanger, M. le Maire, M. Bonhivers, S. Dubois, M. Desmadril, L. Letellier, Purification and structural and functional characterization of FhuA, a transporter of the *Escherichia coli* outer membrane, Biochemistry 35 (1996) 14216–14224.
[15] L. Plançon, C. Janmot, M. le Maire, M. Desmadril, M. Bonhivers, L. Letellier, P. Boulanger, Characterization of a high-affinity complex between the bacterial outer membrane protein FhuA and the phage T5 protein pb5, J. Mol. Biol. 318 (2002) 557–569.
[16] M. Bonhivers, M. Desmadril, G.S. Moeck, P. Boulanger, A. Colomer-Pallas, L. Letellier, Stability studies of FhuA, a two-domain outer membrane protein from *Escherichia coli*, Biochemistry 40 (2001) 2606–2613.
[17] A. Giuliani, F. Jamme, V. Rouam, F. Wien, J.-L. Giorgetta, B. Lagarde, O. Chubar, S. Bac, I. Yao, S. Rey, C. Herbeaux, J.-L. Marlats, D. Zerbib, F. Polack, M. Réfrégiers, DISCO: a low-energy multipurpose beamline at synchrotron SOLEIL, J. Synch. Rad. 16 (2009) 835–841.
[18] N.P. Cowieson, A.J. Miles, G. Robin, J.K. Forwood, B. Kobe, J.L. Martin, B.A. Wallace, Evaluating protein:protein complex formation using synchrotron radiation circular dichroism spectroscopy, Proteins 70 (2008) 1142–1146.
[19] L. Whitmore, B.A. Wallace, DICHROWEB, an online server for protein secondary structure analyses from circular dichroism spectroscopic data, Nucleic Acids Res. 32 (2004) 668–673.
[20] L. Whitmore, B.A. Wallace, Protein secondary structure analyses from circular dichroism spectroscopy: methods and reference databases, Biopolymers 89 (2008) 392–400.
[21] J.G. Lees, A.J. Miles, F. Wien, B.A. Wallace, A reference database for circular dichroism spectroscopy covering fold and secondary structure space, Bioinformatics 22 (2006) 1955–1962.

[22] A. Perczel, M. Hollosi, G. Tusnady, G.D. Fasman, Convex constraint analysis: a natural deconvolution of circular dichroism curves of proteins, Protein Eng. 4 (1991) 669—679.

[23] N.J. Greenfield, Using circular dichroism collected as a function of temperature to determine the thermodynamics of protein unfolding and binding interactions, Nat. Protoc. 1 (2006) 2527—2535.

[24] J.G. Lees, B.A. Wallace, Synchrotron radiation circular dichroism and conventional dichroism spectroscopy: a comparison, Spectroscopy 16 (2002) 121—125.

[25] M. Bonhivers, A. Ghazi, P. Boulanger, L. Letellier, FhuA, a transporter of the Escherichia coli outer membrane, is converted into a channel upon binding of bacteriophage T5, EMBO J. 15 (1996) 1850—1856.

[26] G.S. Moeck, P. Tawa, H. Xiang, A.A. Ismail, J.L. Turnbull, J.W. Coulton, Ligand-induced conformational change in the ferrichrome-iron receptor of Escherichia coli K-12, Molec. Microbiol. 22 (1996) 459—471.

[27] H. Hiramatsu, T. Kitagawa, FT-IR approaches on amyloid fibril structure, Biochim. Biophys. Acta 1753 (2005) 100—107.

[28] S. Krimm, J. Bandekar, Vibrational spectroscopy and conformation of peptides, polypeptides, and proteins, Adv. Prot. Chem. 38 (1986) 181—364.

[29] R. Karlsson, P.S. Katsamba, H. Nordin, E. Pol, D.G. Myszka, Analyzing a kinetic titration series using affinity biosensors, Anal. Biochem. 349 (2006) 136—147.

[30] H.G. Killmann, G. Videnov Jung, H. Schwarz, V. Braun, Identification of receptor binding sites by competitive peptide mapping: phages T1, T5, and phi 80 and colicin M bind to the gating loop of FhuA, J. Bacteriol. 177 (1995) 694—698.

[31] G. Carmel, J.W. Coulton, Internal deletions in the FhuA receptor of Escherichia coli K-12 define domains of ligand interactions, J. Bacteriol. 173 (1991) 4394—4403.

[32] V. Braun, FhuA (TonA), the career of a protein, J. Bacteriol. 191 (2009) 3431—3436.

[33] J.D. Faraldo-Gomez, M.S. Sansom, Acquisition of siderophores in gram-negative bacteria, Nat. Rev. Mol. Cell Biol. 4 (2003) 105—116.

[34] S. Spinelli, A. Desmyter, C.T. Verrips, H.J.W. de Haard, S. Moineau, C. Cambillau, Lactococcal bacteriophage p2 receptor-binding protein structure suggests a common ancestor gene with bacterial and mammalian viruses, Nat. Struct. Mol. Biol. 13 (2006) 85—89.

[35] S. Spinelli, V. Campanacci, S. Blangy, S. Moineau, M. Tegoni, C. Cambillau, Modular structure of the receptor binding proteins of Lactococcus lactis phages. The RBP structure of the temperate phage TP901-1, J. Biol. Chem. 281 (2006) 14256—14262.

[36] S. Ricagno, V. Campanacci, S. Blangy, S. Spinelli, D. Tremblay, S. Moineau, M. Tegoni, C. Cambillau, Crystal structure of the receptor-binding protein head domain from Lactococcus lactis phage bIL170, J. Virol. 80 (2006) 9331—9335.

[37] D. Veesler, C. Cambillau, A common evolutionary origin for tailed-bacteriophage functional modules and bacterial machineries, Microbiol. Mol. Biol. Rev. 75 (2011) 423—433.

[38] M. Zweig, D.J. Cummings, Structural proteins of bacteriophage T5, Virology 51 (1973) 443—453.

[39] M. Mondigler, T. Holz, K.J. Heller, Identification of the receptor-binding regions of pb5 proteins of bacteriophages T5 and BF23, Virology 219 (1996) 19—28.

[40] W. Rabsch, L. Ma, G. Wiley, F.Z. Najar, W. Kaserer, D.W. Schuerch, J.E. Klebba, B.A. Roe, J.A. Laverde Gomez, M. Schallmey, S.M. Newton, P.E. Klebba, FepA- and TonB-dependent bacteriophage H8: receptor binding and genomic sequence, J. Bacteriol. 189 (2007) 5658—5674.

[41] J. Hong, K.P. Kim, S. Heu, S.J. Lee, S. Adhya, S. Ryu, Identification of host receptor and receptor-binding module of a newly sequenced T5-like phage EPS7, FEMS Microbiol. Lett. 289 (2008) 202—209.

[42] M. Kim, S. Ryu, Characterization of a T5-like coliphage, SPC35, and differential development of resistance to SPC35 in Salmonella enterica serovar typhimurium and Escherichia coli, Appl. Environ. Microbiol. 77 (2011) 2042—2050.

[43] K.J. Heller, H. Schwarz, Irreversible binding to the receptor of bacteriophages T5 and BF23 does not occur with the tip of the tail, J. Bacteriol. 162 (1985) 621—625.

[44] J. Garnier, D.J. Osguthorpe, B. Robson, Analysis of the accuracy and implications of simple methods for predicting the secondary structure of globular proteins, J. Mol. Biol. 120 (1978) 97—120.